

Figure Legends.

Figure S1. *XAL2* is expressed in different cell types of *A. thaliana* roots. (A) Expression data for *XAL2* in different tissues of the root recovered from cell sorting published data (Data analysed from Birnbaum and collaborators (2003) and Nawy and collaborators (2005)). (B-H) *In situ* hybridization of lateral root primordia at different developmental stages (A-G); H is the negative sense control. See Experimental procedures for details of the procedures used.

Figure S2. *XAL2* is highly expressed during lateral root development. *p1KbXAL2:XAL2-GUS* lines grown for 5 d.p.s. and then stained for GUS reaction for 24 hours.

Figure S3. *xa/2-2* exhibits normal cell cycle duration and does not alter *CYCB1;1_{DB}:GUS* expression. (A) Cell cycle duration (calculation for this parameter is described in detail in Experimental procedures). The data was analyzed with the JMP 5.1.1 version statistical package. (B) Nomarski photographs of *CYCB1;1_{DB}:GUS* expression of 7 d.p.s wild-type and *xa/2-2* mutant plants (100%; *n*=47) (Bar = 50 μ m).

Figure S4. *xa/2-2* has an altered development of the stele with modified anticlinal radial division of the pericycle cells and no effect on total stele width. (A) A scheme showing how the stele development was analyzed. Horizontal lines are drawn at the levels of the 1st and 5th cortical (including initial) cells above the QC (*); at these levels Z-confocal scanning was performed and the transverse sections were reconstructed and analyzed. (B and C) Quantitative analysis of the stele development in wild-type and *xa/2-2* plants. (B) The stele diameter and (C) the number of pericycle cells in wild-type and *xa/2-2* in the transverse optical section at the level of the first and the fifth cortical cells. Mean \pm SD (*n* = 7-10 for the stele diameter and *n*= 6-9 for the number of pericycle cells); statistical

differences at $P < 0.01$ (**) and $P < 0.001$ (***) are shown. (D and E) Transverse sections made in wild-type (Col-0) and *xa/2-2* mutant of live roots 4 d.p.s. at the level of the 1st and 5th cortical (including initial) cells above the QC. The images were enhanced using Gaussian Blur and Unsharp Mask filters and analyzed with the Image J software. Yellow and red circles indicate the cortex and pericycle cells, respectively (Bar = 10 μm). (F) Histological cross sections of wild-type and *xa/2-2* plants ($n=10$). (G) Width of root and stele of 4 d.p.s. wild-type and *xa/2-2* plants ($n=29$).

Figure S5. XAL2 does not regulate the QC identity genes, *WOX5*, *SCR*, and *PLT1*, but affect the domain of expression of *QC25*. Confocal image of longitudinal optical sections of meristem roots at 5 d.p.s. for *WOX5:GFP* expression (100%; $n=23$) and *SCR:GFP* expression (100%; $n=70$); red signal is emitted by propidium iodide that was used as a counterstain. Nomarski optics images of cleared roots of *PLT1-GUS* (100%; $n=20$) and *QC25* marker lines at 7 d.p.s. plants (80%; $n=44$). White arrowhead indicates the position of the QC in all cases (Bar = 50 μm).

Figure S6. XAL2 expression is induced by auxin treatment but XAL2 does not affect auxin signaling. (A) Nomarski optics images of longitudinal sections of wild-type and *xa/2-2* of 6 d.p.s. roots expressing *pDR5-GUS* under auxin treatment (75%; $n=80$) (Bar = 50 μm). (B) qRT-PCR analysis of *GH3*, *IAA1*, *IAA2*, *IAA7* and actin expression in 5 d.p.s. wild-type and *xa/2-2* plants. Bars represent standard errors (SE).

Figure S7. XAL2 up-regulates *PIN1* gene expression. *pPIN1-GFP* optical sections ($n=10$) of 4 d.p.s. wild-type and *xa/2-2* mutant plants. Horizontal lines are drawn at the QC, at the 1st and at the 5th cortical (including initial) cells above the QC (*).

Figure S8. XAL2 does not affect the expression of PIN2 or PIN7. (A) *pPIN7::PIN7-GFP* expression in wild-type and *xal2-2* mutant plants. *PIN7* expression has two overlapping domains of expression; one of them expanded is present in provascular tissues in 54% of the *xal2-2* plants and in 62% of the wild-type plants ($n=40$). (B) *pPIN2::PIN2-GFP* (100%; $n=30$) expression in roots of wild-type and mutant *xal2-2* plants. Confocal images of longitudinal optical sections of root meristem with propidium iodide as a red counterstain are shown (Bar = 50 μ m). In both cases the plants were 4 d.p.s. old.

Figure S9. 35S:XAL2-GFP is localized in nuclei and cytoplasm in Arabidopsis root cells. Longitudinal confocal sections of different parts of Arabidopsis root tips of 4 d.p.s. *35S:GFP-XAL2* plants ($n=10$). Propidium iodide was used as a red counterstain (Bar = 50 μ m).

Figure S10. Loss of function of XAL2 and PIN1 affect ABCB19 expression. qRT-PCR analysis of *ABCB19* expression with or without IAA treatment in *xal2-2* and *pin1-5* normalized with wild-type plants. * Marks that the change is significant at $P<0.001$ by Student's t test followed by Neuman Keuls post hoc ANOVA.

TableS1. Primer sequences for RT-PCR experiments (5'-3' direction).

pPIN1-F3	CAC GAA TTT TAG TGA TTG ATG TT
pPIN1-R3	TTT GGG TTC TCT AAA AGG CTG
pPIN1-F2.1	AAT TTC ATG CAG TTG TAT ACG G
pPIN1-R2.1	GGA CTG TCT ACG GTG GAA GC
pPIN1-F2	GCC GTG TTA AAA ATT CAA TTC T
pPIN1-R2	GCT TAC ACA AAT CAG TCT GAT G

pPIN1-F1	CAC ACA CTA TTA TGT TGG AAT G
pPIN1-R1	GTC ATA ACG TGG TAG AAG TCC G
pPIN1-IF1	GTC AGC CTT GAA TGC GTA TAT G
pPIN1-IR1	CAT GCT TCC ACA TGA TTT GTT T
pPIN1-IF2	CCC TTG AAT AGG AGG AAC CAT T
pPIN1-IR2	AAA GCT GCT CTT CTG TTT CCA C
En8130	GAG CGT CGG TCC CCA CAC TTC TAT AC
XAL2F	TGT AAC GTT TAC ATT GTA AGC G
XAL2R	AGA ATT GAG AAC ATA AAT CAG C
up-p14-FW	CACC-TCT TGT CCG AGA GGA GCT GGC A
Atg-14-RV (+NcoI)	TCT TTC CCC TCA CCA TGG TTC TAA TT
XAL2F1	GTA GAA AGA TAT CAA AAG CGA A
XAL2R2	GGA GGA AAC TTT TTG AAG TGT
PIN1F	CAG ATG CAG GTC TAG GCA TGG
PIN1RT	GG GCA ACG CGA TCA ACA TCC
TUB2F	AGG ACT CTC AAA CTC ACT ACC
TUB2R	TCA CCT TCT TCA TCC GCA GTT
qGH3_1019_F	TCA ATC CTA TGT GCA AGC CTG
qGH3_1334_R	TTT GCG TTA TTC ACC GCC T
qIAA1_L_85	CTT TCT TGC GTC AGA AGC AAC
qIAA1_R_424	CGA CCA ACA TCC AAT CTC CA
qIAA2_L_3	GGC GTA CGA GAA AGT CAA CGA
qIAA2_R_324	TAA CGC TTT GAG AAG CTC GG
qIAA7_L_157	GAA GGC TCC GTT GAT CTC AA
qIAA7_R_480	GCT GAA CAT TTT GGC CAA TGC
qPIN1F	CGT GGA GAG GGA AGA GTT TA
qPIN1R	AAC ATA GCC ATG CCT AGA CC

qPIN2F	TAT CAA CAC TGC CTA ACA CG
qPIN2R	GAA GAG ATC ATT GAT GAG GC
qPIN4F	ACA ACG CCG TTA AAT ATG GA
qPIN4R	AGA CCC CAT TTT ATT CAG CC
qTUBF	TGG GAA CTC TGC TCA TAT CT
qTUBR	GAA AGG AAT GAG GTT CAC TG
XAL3F	ATT GAG AAG TTG AAG GCA GA
XAL3R	ACG TTG ATT GTG ATG ATG C
UBIF	CTT CGT CAA GAC TTT GAC CG
UBIR	CTT CTT AAG CAT AAC AGA GAC GAG
AO4F	GGC TGC AGT GGT CAC TTT TGT AGT TGG AG
AO9R	CAT GCC ATG GGA TAG CGT TCA ATT GTT G
ARF5F	TCG CAG ATC ACA TCA GCT AGC
ARF5R	GGT TTC TCC TCT ACC AGT TGG

Materials and Methods.

Plant Materials, DNA constructs and Growth Conditions. *Arabidopsis thaliana* wild-type and *xa12-2* lines, *pPIN2:PIN2-GFP*, *pPIN7:PIN7-GFP* and *DR5-GUS* auxin reporter lines are in Col-0 genetic background. *pPIN2:PIN2-GFP* and *pPIN7:PIN7-GFP* were obtained from B. Scheres; *CYCB1;1_{DB}-GUS* was obtained from P. Doerner. For the *35S:GFP-XAL2* construct, an (*AGL14*) *XAL2* cDNA entry clone (de Folter *et al*, 2005) was recombined using the Gateway system (Invitrogen) in the pK7WG2 destination vector (Karimi *et al*, 2002). In the case of the *35S:XAL2* construct an (*AGL14*) *XAL2* cDNA entry clone (de Folter *et al*, 2005) was recombined using the Gateway system (Invitrogen) in the pH7WG2 destination vector (Karimi *et al*, 2002).

Hormone Treatments. Plants were grown for 7 days in hormone-free medium plates and then transferred to growth media supplemented with 1 μ M of IAA (Indole Acetic Acid) for 4 hours. After IAA treatment, seedlings of *DR5:GUS* were subject to GUS reaction for 40 min at room temperature; stained plants were cleared and visualized under a microscope. For Real Time PCR expression analysis 5d old seedling of wild-type and *xa12-2* plants were treated with 0.001%DMSO in water (control) or 1 μ M IAA for 2h (Murphy and Taiz, 1995).

GUS staining. Plant material for light microscopy and GUS staining was prepared as previously described by Malamy and Benfey (1997) and visualized under a microscope (see below). Seedlings were subjected to GUS reaction overnight at 37°C for *CYCB1:GUS*. To restrict the diffusion of GUS blue staining, 2mM of $K_3FE(CN)_6$ and $K_4FE(CN)_6$ were added.

Quantitative Analysis of Cellular Parameters of Root Growth. The average cell cycle time for cortical cells and cell production in plants growing between 7-8 days was evaluated for plants grown in 0.2 x MS medium supplemented with 2% sucrose, using the rate of cell production method (Ivanov and Dubrovsky, 1997). Briefly, the duration of the cell cycle (T) was calculated for each individual root using the equation: $T = (\ln 2 N_m I_e) V^{-1}$, where N_m is

the number of meristematic cells in one file of the cortex, l_e , is the length of fully elongated cells calculated as the average length of ten fully elongated cortex cells in the same root and V is the root growth rate calculated as $\mu\text{m h}^{-1}$.

Real-Time quantitative PCR. Seedlings were grown as described by Murphy and Taiz (1995). RNA extraction and PCR conditions were as described by Blakeslee and collaborators, (2004). See <http://www.hort.purdue.edu/hort/research/murphy/protframe.htm> for complete details and Table S1 for primer sequences. Primer sequences for quantitative PCR are marked with a “q” at the beginning of the name of the primer. The qRT-PCR data were prepared using the value of the wild type against the standard compared to the value of *xaI2-2* against the standard for genes *GH3*, *IAA1*, *IAA7*, *IAA2*, *ABCB19* and *alpha actin*. In these experiments the standard deviations are the sum of standard deviations. For qRT-PCR of *ABCB19* with or without IAA we used the ABI program with a SD threshold for three replicates to <0.16 ; if data are ≥ 0.16 , they are not significant. Quantification and data acquisition was done using iCycler Real Time system (Biorad) using Syber Green I as a fluorophor. Realtime PCR was run using 1:50 dilution of first strand at 95°C for 40s (denaturation), 54°C for 40s (annealing) and 72°C for 20s (extension) for 35 cycles. Analysis was according to the $2^{-\Delta\Delta\text{CT}}$ method (Livak and Schmittgen, 2001).

mRNA “*in situ*” hybridization experiments. The roots were fixed in 4% paraformaldehyde, vacuum-infiltrated and kept overnight at 4°C . Samples were then dehydrated through an ethanol series, passed through an ethanol:Histoclear (National Diagnostics) series and embedded in Paraplast+ (Oxford Labware). Microtome sections ($9\ \mu\text{m}$) of the samples were mounted on Probe-On Plus Slides (Fisher Scientific). The roots can be stored at the refrigerator (4°C) in 70% ethanol until *in situ* hybridization. Digoxigenin-labeled probes were synthesized following the manufacturer's instructions (Boehringer Mannheim) and hydrolyzed to an average length of 200 bp. Probes were chosen to avoid the presence of the MADS-box sequence and to avoid cross-hybridization with other MADS-box mRNAs.

Microscopy. Plant material for light microscopy was rehydrated for five days in each one of the ethanol steps modifying Malamy and Benfey protocol (1997). GFP samples were scanned without fixation. Roots were visualized using Nomarski optics under an Olympus BX60 microscope and photographed with a Leica camera. Confocal images were acquired using an inverted Zeiss LSM 510 Meta microscope (Carl Zeiss, Oberkochen, Germany) with a dry 40x and a water immersion 63X C-Apochromat objective after root tissue was stained with 10 μ M propidium iodide.

References.

- Birnbaum K, Shasha DE, Wang JY, Jung JW, Lambert GM, Galbraith DW, Benfey PN (2003) A gene expression map of the Arabidopsis root. *Science* **12**: 1956-60
- Blakeslee JJ, Bandyopadhyay A, Peer WA, Makam SN, Murphy AS (2004) Relocalization of the PIN1 auxin efflux facilitator plays a role in phototropic responses. *Plant Physiol.* **134**: 28-31
- de Folter S, Immink RG, Kieffer M, Parenicová L, Henz SR, Weigel D, Busscher M, Kooiker M, Colombo L, Kater MM, Davies B, Angenent GC (2005) Comprehensive interaction map of the Arabidopsis MADS Box transcription factors. *Plant Cell* **17**: 1424-33
- Ivanov VB, Dubrovsky JG (1997) Estimation of the cell-cycle duration in the root apical meristem: a model of linkage between cell-cycle duration, rate of cell production, and rate root growth. *Int J Plant Sci* **158**: 757-763
- Karimi M, Inzé D, Depicker A (2002) GATEWAY vectors for Agrobacterium-mediated plant transformation. *Trends Plant Sci* **7**: 193-5
- Livak KJ, Schmittgen TD (2001) Analysis of relative gene expression data using real-time quantitative PCR and the 2(-Delta Delta C(T)) *Methods* **25**: 402-8
- Malamy JE, Benfey PN (1997) Organization and cell differentiation in lateral roots of Arabidopsis thaliana. *Development* **124**: 33-44
- Murphy A, Taiz L (1995) A new vertical mesh transfer technique for metal-tolerance studies in Arabidopsis-ecotypic variation and copper-sensitive mutants. *Plant Physiology* **108**: 29-38
- Nawy T, Lee JY, Colinas J, Wang JY, Thongrod SC, Malamy JE, Birnbaum K, Benfey PN (2005) Transcriptional profile of the Arabidopsis root quiescent center. *Plant Cell* **17**: 1908-25

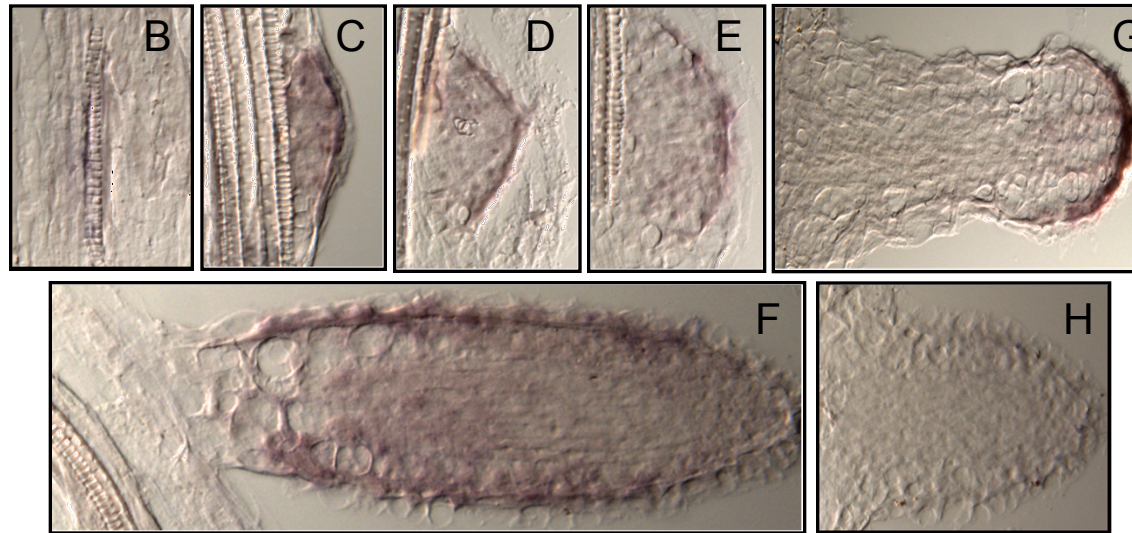
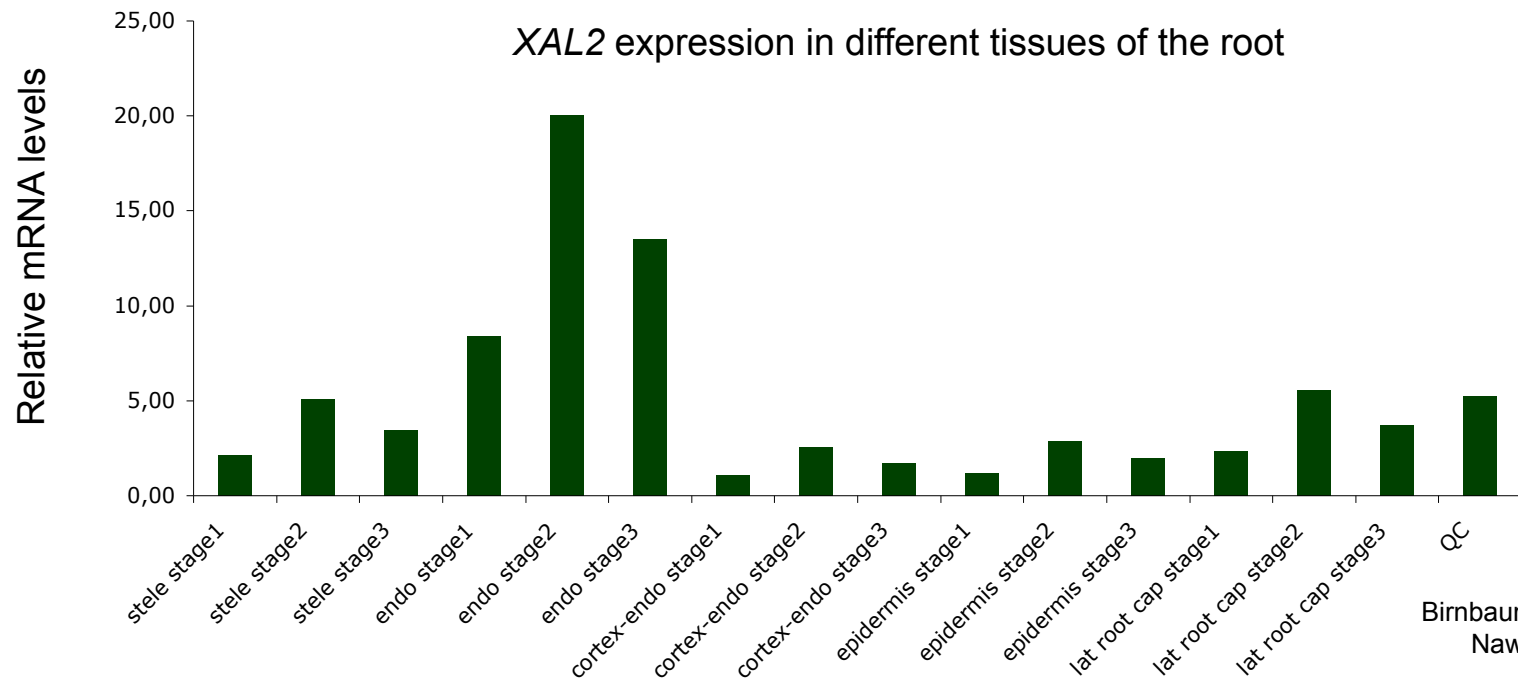
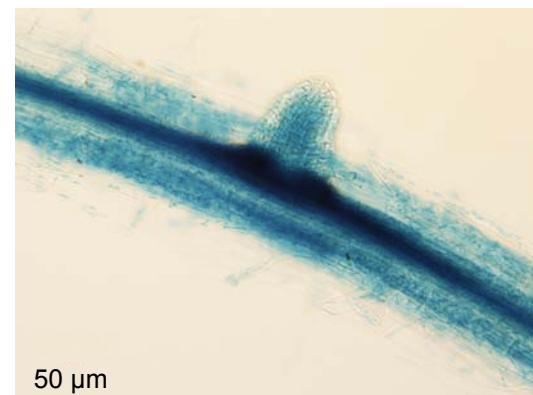
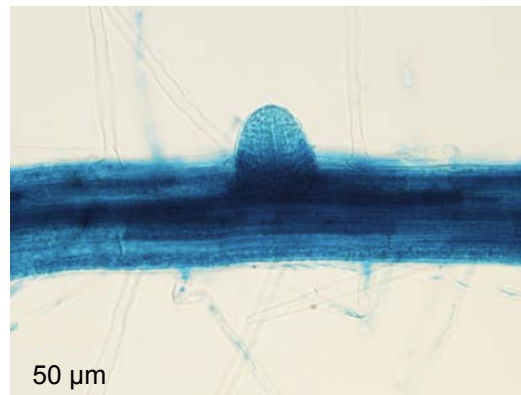
A

Figure S1



1kbXAL2:XAL2-GUS

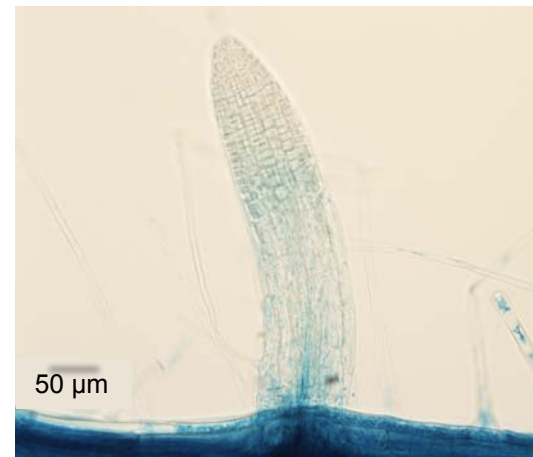
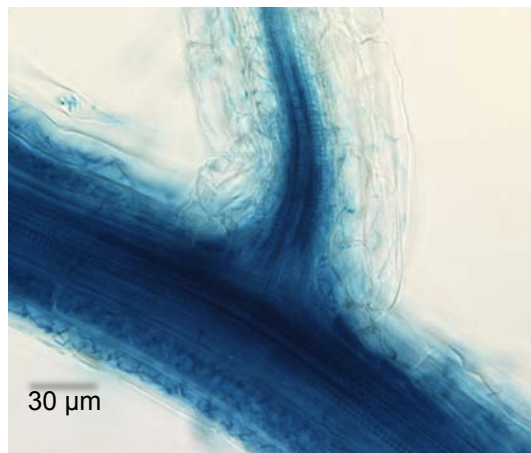
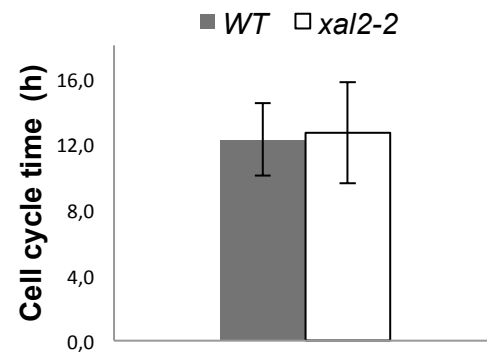


Figure S2

A



B

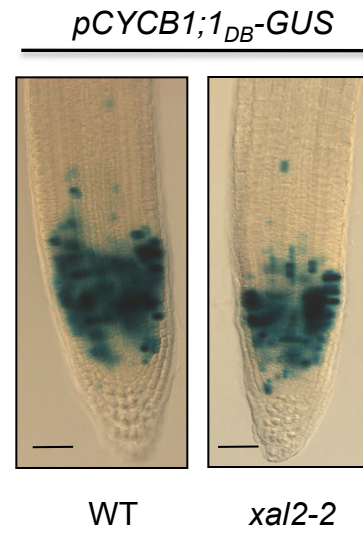


Figure S3

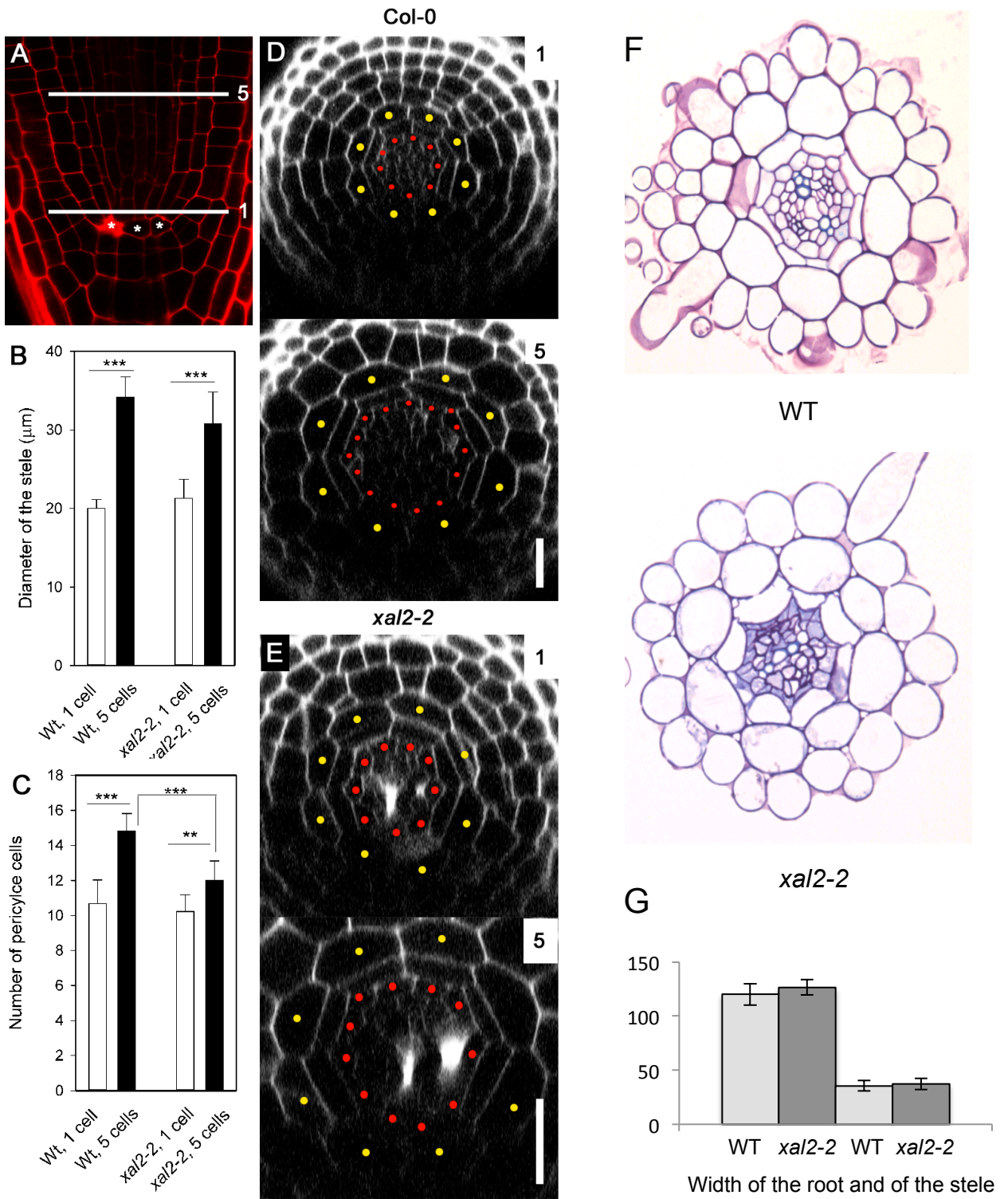


Figure S4

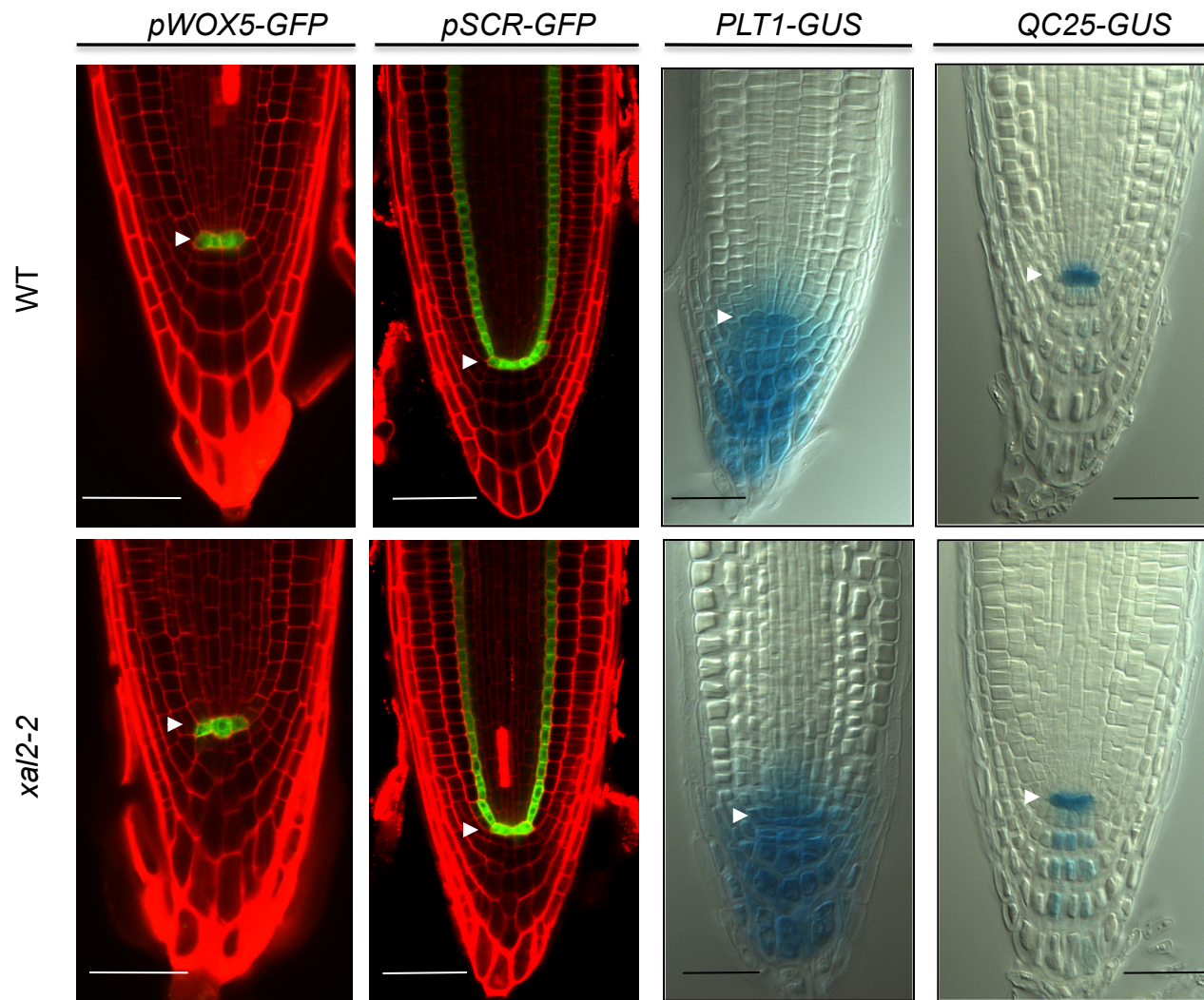


Figure S5

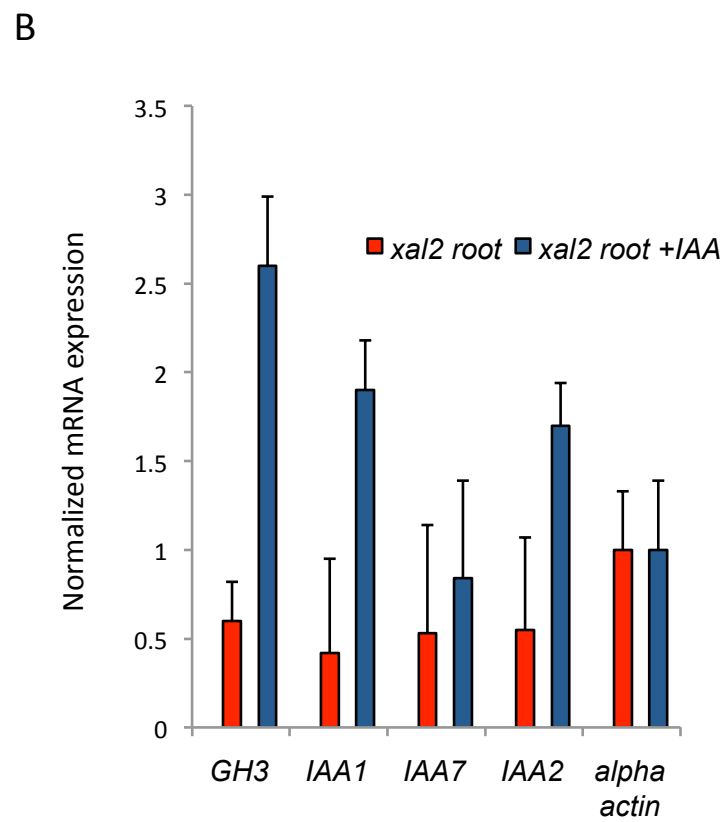
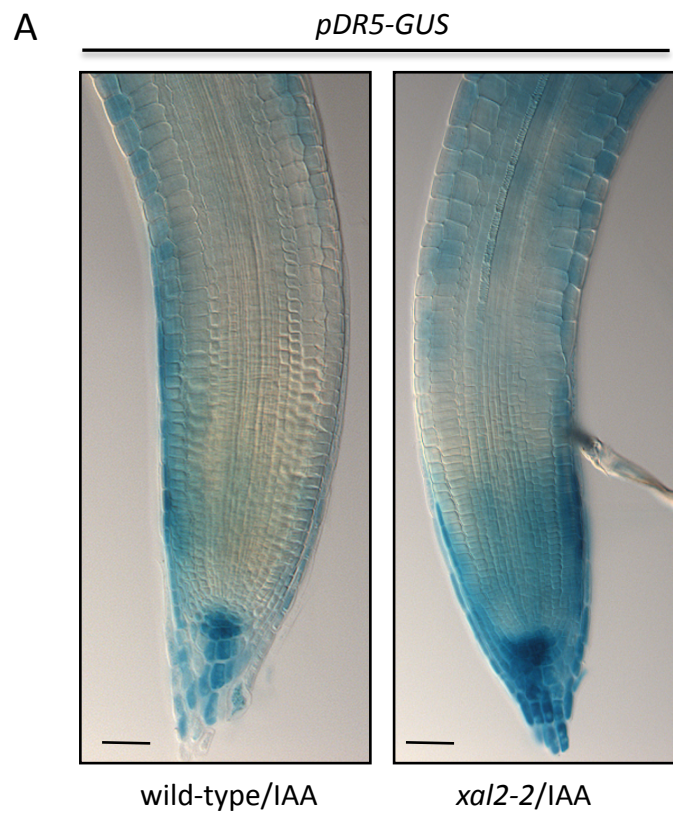


Figure S6

pPIN1-GFP

WT

xal2-2

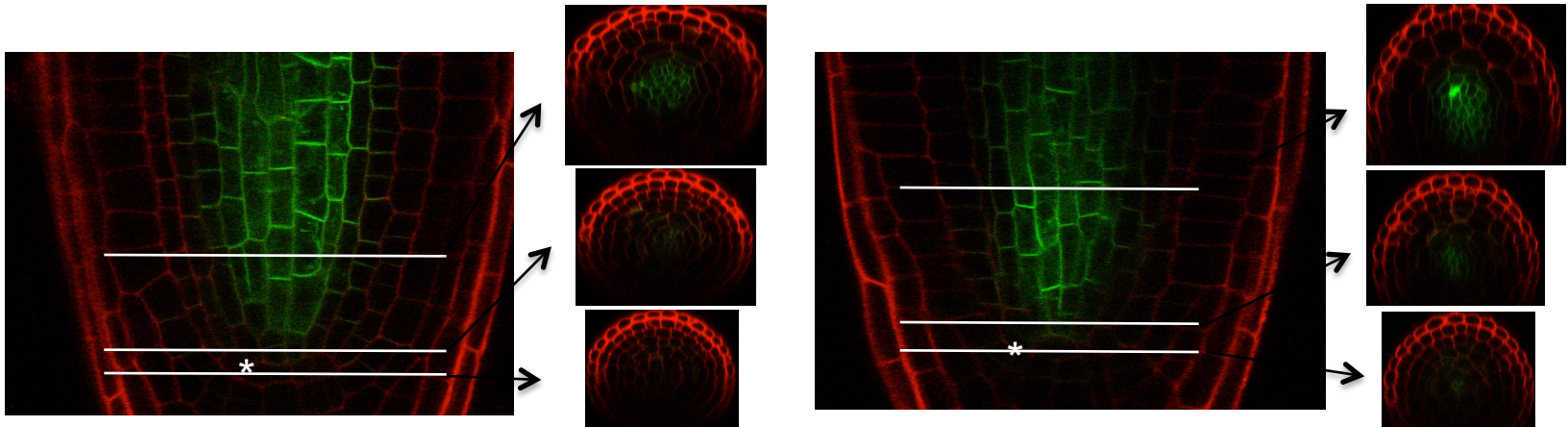
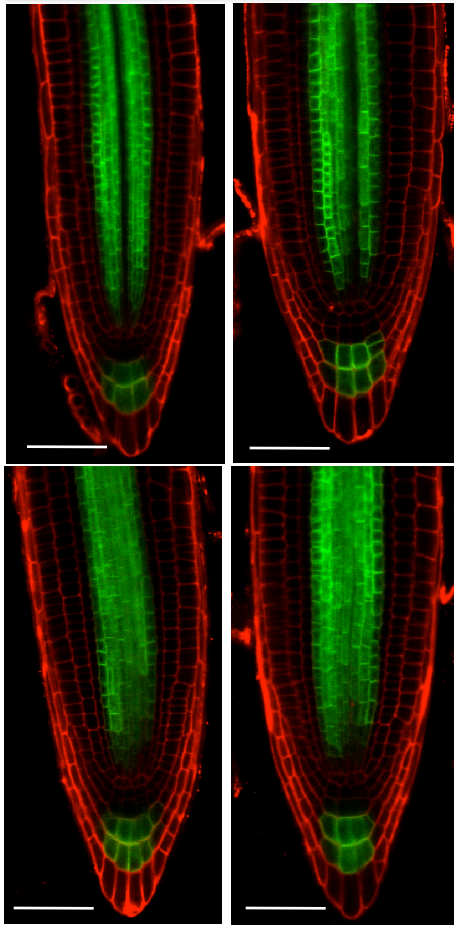


Figure S7

A

pPIN7::PIN7-GFP

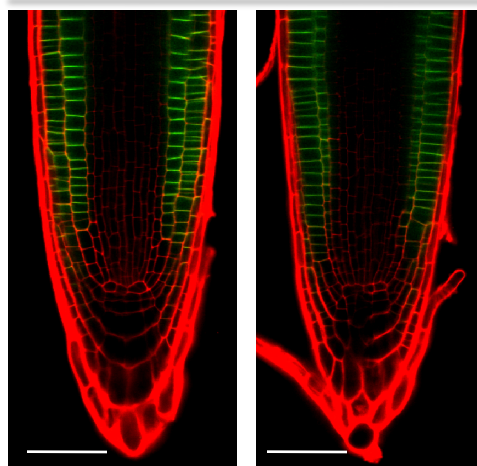


WT

xal2-2

B

pPIN2::PIN2-GFP



WT

xal2-2

35S-GFP:XAL2

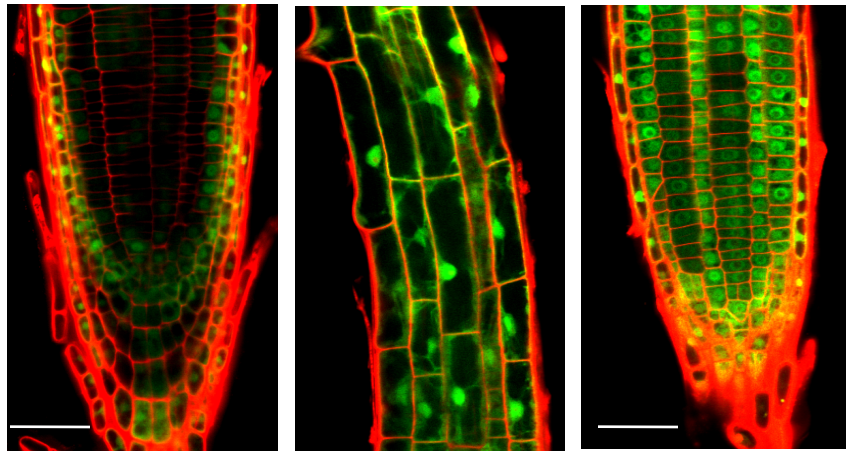


Figure S9

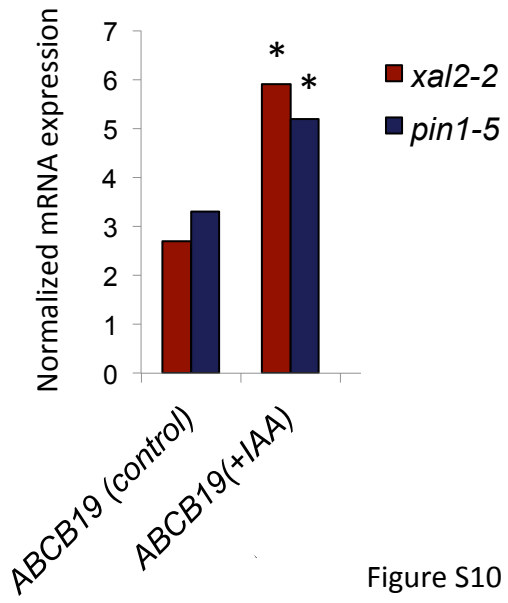


Figure S10